P8.23
DEVELOPMENT AND INTERCOMPARISON OF AMSU RAIN RATE ALGORITHMS

Ryan Aschbrenner, Grant W. Petty

Department of Atmospheric and Oceanic Sciences, Universtiy of Wisconsin-Madison

Hung-Lung Huang

Cooperative Institute for Meteorological Satellite Studies, University of Wisconsin-Madison

1. INTRODUCTION

Satellite remote sensing has become the primary method of precipitation monitoring over much of the earth, and microwave-based satellite retrievals have rapidly advanced over the past two decades. The Advanced Microwave Sounding Unit (AMSU), first launched in 1998, includes channels at 89 and 150 GHz that are well-suited for detecting the signatures of precipitation. Data from these channels have shown great promise both for delineating the areal extent of precipitation and for estimating the precipitation rate. In particular, these frequencies allow for retrievals over land surfaces; this sets them apart from lower frequency algorithms which are designed to detect the emission signature associated with rainfall in the marine environment.

The objective of this study is to evaluate and intercompare three over-land precipitation detection methods developed for the AMSU. Algorithm performance and calibration is evaluated based on the Heidke skill score applied to matchups between radar- and AMSU-derived rain rates. The purpose is to select an AMSU algorithm that is adequate for real-time precipitation monitoring over much of North America.

2. DATA AND ALGORITHMS

Data collected by AMSU on board the NOAA-16 polar orbiting satellite were collected for the period covering November 2002 through September 2003 in order to achieve a substantial sample size and to assess the effect of seasonality on AMSU precipitation retrievals. WSR-88D NEXRAD data were also archived for use as a ground benchmark after being co-located and convolved to the AMSU resolution on a pixel-by-pixel basis.

Corresponding author address:
R. Aschbrenner, AER, Inc., 131 Hartwell Ave., Lexington, MA 02421; e-mail: raschbre@aer.com

Two general algorithmic approaches to rain rate retrieval were considered, but each is linked to the microwave scattering signature of frozen hydrometeors in the upper parts of most midlatitude rain clouds. The first of these approaches, adopted by the NESDIS Microwave Surface and Precipitation Products System (MSPPS) team, is based on a physical model of the relationship between the microwave signature of ice aloft and the corresponding surface rain rate. Details of this algorithm are presented in Weng and Grody (2000) and Zhao and Weng (2002). The basis for this algorithm is a scattering parameter (denoted by Ω), which measures the brightness temperature difference between an AMSU measurement taken in the presence of precipitation and a modeled precipitation-free measurement of the same scene. An ice water path product is derived from Ω, and, as a final step, rain rates are computed as a function of ice water path based on cloud modeling results.

The other general retrieval methodology is empirical and serves as the basis for our two in-house algorithms. These were developed as simple experimental alternatives to the NESDIS algorithm. They rely on climatological mean T_b values observed by selected AMSU-B channels; the climatological mean (computed at monthly intervals) serves as a background on which to compare individual AMSU swaths. The goal is to identify individual pixels that display a significant negative departure in T_b at frequencies most sensitive to hydrometeor scattering. The 89 and 150 GHz channels are useful in precipitation monitoring studies because of their sensitivity to lower atmospheric features, and were therefore included in the climatological algorithm component of this study.

One algorithm is based solely on the 150 GHz channel, and the precipitation signature is captured using the formula

$$\delta T_1 = \overline{T_{b,150}} - T_{b,150}, \qquad (1)$$

where δT_1 is the T_b depression, $\overline{T_{b,150}}$ is the monthly mean T_b for a local two degree grid box, and $T_{b,150}$ is simply the AMSU-measured T_b for the pixel in question. Thus a positive value of δT_1 represents a T_b depression. Precipitation generally creates T_b depressions ranging from 15 K to approximately 150 K; smaller depressions are more likely caused by natural variability.

The second climatology algorithm relies on the assumption that the 89 and 150 GHz channels respond to precipitating scenes differently than they respond to clear scenes, and the precipitation signature is described by the formula

$$\delta T_2 \quad = \quad (\overline{T_{b,150}} - \overline{T_{b,89}}) - (T_{b,150} - T_{b,89}) = \overline{\delta T} - \delta T,$$

where the barred terms represent monthly mean values, and the unbarred terms represent individual AMSU measurements. In precipitation, the scattering of upwelling radiation by ice particles was typically observed to depresses $T_{b,150}$ below $T_{b,89}$. Thus δT tends to be significantly less than zero in precipitation. In a clear scene over ocean, δT tends to be greater than zero due to the strong response of $T_{b,150}$ to water vapor emission; this is particularly true in the tropics or other regions experiencing high humidity. In a clear scene over land, δT tends to be approximately equal to zero as both 89 and 150 GHz respond to the highly emissive land surface rather than the weaker water vapor signal. Thus δT_2 is positive in precipitation and negative or near-zero in clear scenes.

3. STRATEGY FOR CALIBRATION

The Heidke skill score (HSS) is a measure of the skill (relative to chance) of a method used to make a binary classification and is obtained via a formula applied to a 2 contingency table (columns represent "yes" or "no" according to the algorithm and rows represent "yes" or "no" according to the "truth" data set). Applied to satellite rainfall estimation, the HSS has sometimes been utilized to characterize the performance of an algorithm at distinguishing rain from no rain, as compared to a validation data set such as radar.

Conner and Petty (see Conner and Petty (1998)) pointed out a problem with applying the skill score to precipitation verification based on the mere presence or absence of rain. In particular, the threshold of sensitivity of the estimation method may be incompatible with the validation method, so that that the resulting single-value HSS is misleading. They proposed instead to compute HSS as a function of two continuously varying thresholds of rainfall rate, one applied to the validation data and the other applied to the retrieval. This allows one to evaluate the *maximum* skill with which a particular algorithm can distinguish rain rates greater than *any* arbitrary threshold applied to the validation data. Among other things, this method allows the "intrinsic" skill of the algorithm to be evaluated independently of any systematic calibration errors, a feature not shared by a standard performance measure such as the RMS error. Moreover, the maximum skill for a particular validation threshold is invariant with respect to non-linear calibration errors, unlike the case for the linear correlation coefficient.

The maximum HSS is identified by dividing the range of radar-derived rain rates and AMSU-derived rain rates (or T_b depressions, as in the case of the climatology-based algorithms) each into 100 equal intervals and computing the HSS for all combinations of radar and algorithm thresholds. In this way, the HSS is computed as a two-dimensional function of varying algorithm and verification thresholds. The radar-derived rain rates are divided into intervals beginning at 0 and extending to 10 mm hr^{-1} while the algorithm-derived rain rates are divided into intervals extending from 0 mm hr^{-1} (or K) to the maximum algorithm output value occurring in the data set. Thus 10 000 scores are computed and the maximum score determines the combination of radar and AMSU thresholds that provides greatest confidence in algorithm performance.

Two-dimensional contour plots of HSS are then created, with NEXRAD thresholds on the ordinate and algorithm thresholds on the abscissa. These plots also identify, for any given NEXRAD threshold, the algorithm threshold that maximizes algorithm skill. This can be taken a step further by identifying HSS maxima for various NEXRAD thresholds and plotting a best-fit line through these maxima points. The best fit line thus identifies the axis of maximum HSS on the two-dimensional contour plot. The HSS contour plot of a robust algorithm will exhibit a linear axis of (high) maximum skill, and this axis would have a slope near unity. If this has a slope significantly less than unity, then one may infer that the algorithm consistently overestimates rain intensity. The best-fit line also serves as a calibration curve which relates algorithm output to NEXRAD-derived rain rate.

4. RESULTS

The training set consisted of all even-numbered dates; calibration curves were derived from these dates, and the calibrations were tested using data from the odd-numbered dates. The calibration established a radar-adjusted NESDIS rain rate product, and it allowed for the conversion of δT_1 and δT_2 into rain rate estimates. Calibration was carried out on both a month-by-month basis, and on the entire data set. HSS contour plots and calibration curves derived from the entire data set

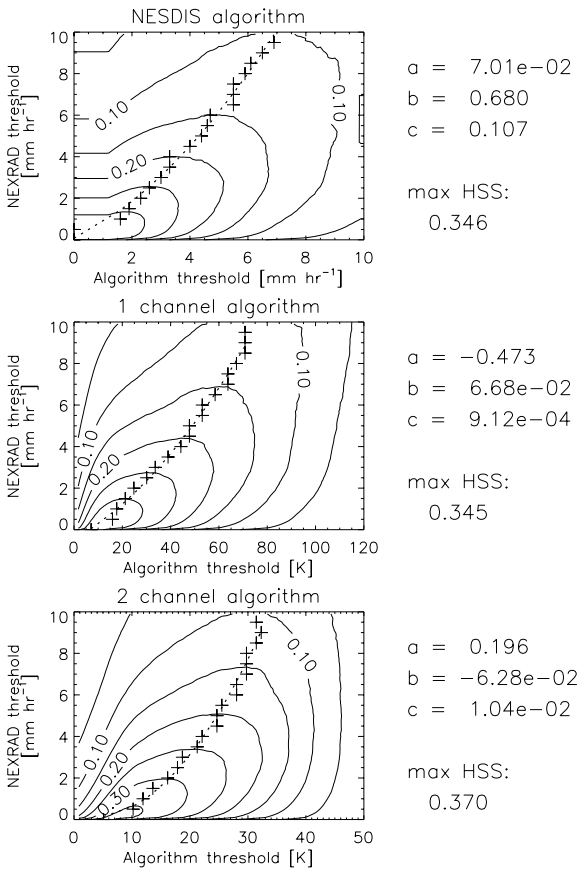

FIG. 1. Heidke skill score contour plots for the entire 11-month data set for the three algorithms. Calibration coefficients and maximum HSS values are listed to the right of each algorithm plot. The + symbols represent points of maximum HSS for various validation thresholds, and the dashed lines are polynomial fits to these points of maximum HSS.

are given in Fig. 1.

The calibrations were evaluated using a technique previously used, for example, by Ferraro and Marks (1995). The NEXRAD rain rates were binned into 1 mm hr^{-1} intervals, and the mean AMSU-derived rain rate was computed within each bin. This analysis therefore examines the sensitivity of the AMSU retrievals to precipitation intensity. The mean AMSU rain rates tended to be highly correlated with the NEXRAD rain rate bins, as correlation coefficients of 0.869, 0.822 and 0.303 were achieved by the NESDIS, one channel and two channel algorithms, respectively. Although all three AMSU algorithms provided nearly perfectly correlated and unbiased mean values for low rain rates, a clear low bias was present in the AMSU retrievals for NEXRAD rain rates above approximately 7 mm hr^{-1}. The radar Z-R relationship may be partly responsible because reflectivities above 50 dBZ correspond to extremely high rain rates. Several high rates averaged within an AMSU pixel may lead to a high bias in the radar retrievals. Subsampling effects produced by the lower AMSU resolution may further enhance the AMSU low bias; the larger sampling area may smooth the hydrometeor scattering signal and cause underestimates at high rain rates.

The low correlation coefficient achieved by the two channel algorithm in this analysis may be attributed in part to coastal effects. Coastal pixels, which contain a fraction of high-emissivity land and lower-emissivity water, caused a high bias in the AMSU rain rate estimate as the algorithm was calibrated only for land surfaces. In a clear scene, the 89 and 150 GHz T_b tend to be similar over land, but the 150 GHz T_b tends consistently exceed the 89 GHz T_b over ocean. Thus, separate land and ocean calibrations would be required. Since the data set is heavily weighted toward light rain events, the inclusion of occasional coastal errors likely compromises the binning analysis results for higher rain rates. Further analysis will require more stringent screening near coastal areas.

Figure 2 shows imagery from 22 Sep 2003 in which all three algorithms are generally successful. Unisys surface maps from 12Z on 22 Sep and 00Z on 23 Sep indicate a surface low near lower Michigan, and an associated cold front sweeping across most of the eastern and southern states. The frontal rain band is unmistakably delineated by the three algorithms, demonstrating that strong hydrometeor scattering is producing an identifiable signature in the AMSU data. There are numerous occurrences of isolated precipitation that were missed by the AMSU algorithms, however. Optimistically, some of these may be due to radar error (e.g. ground clutter). Others may have spatial scales that are below the resolution of the AMSU sensor, and therefore the associated scattering signature is diminished due to subsampling effects. However, in cases of widespread stratiform precipitation (not shown), all algorithms experienced difficulty in resolving the precipitation signature as any associated hydrometeor scattering was too weak to be resolved.

5. CONCLUSIONS

All three algorithms were approximately equally successful in delineating precipitation areal extent over land surfaces. Although the NESDIS algorithm is more physically-based, it apparently does not provide a marked improvement in skill based on the analyses employed in this study. In fairness, the NESDIS algorithm is designed for global application, while the empirical algorithms described herein have been optimized

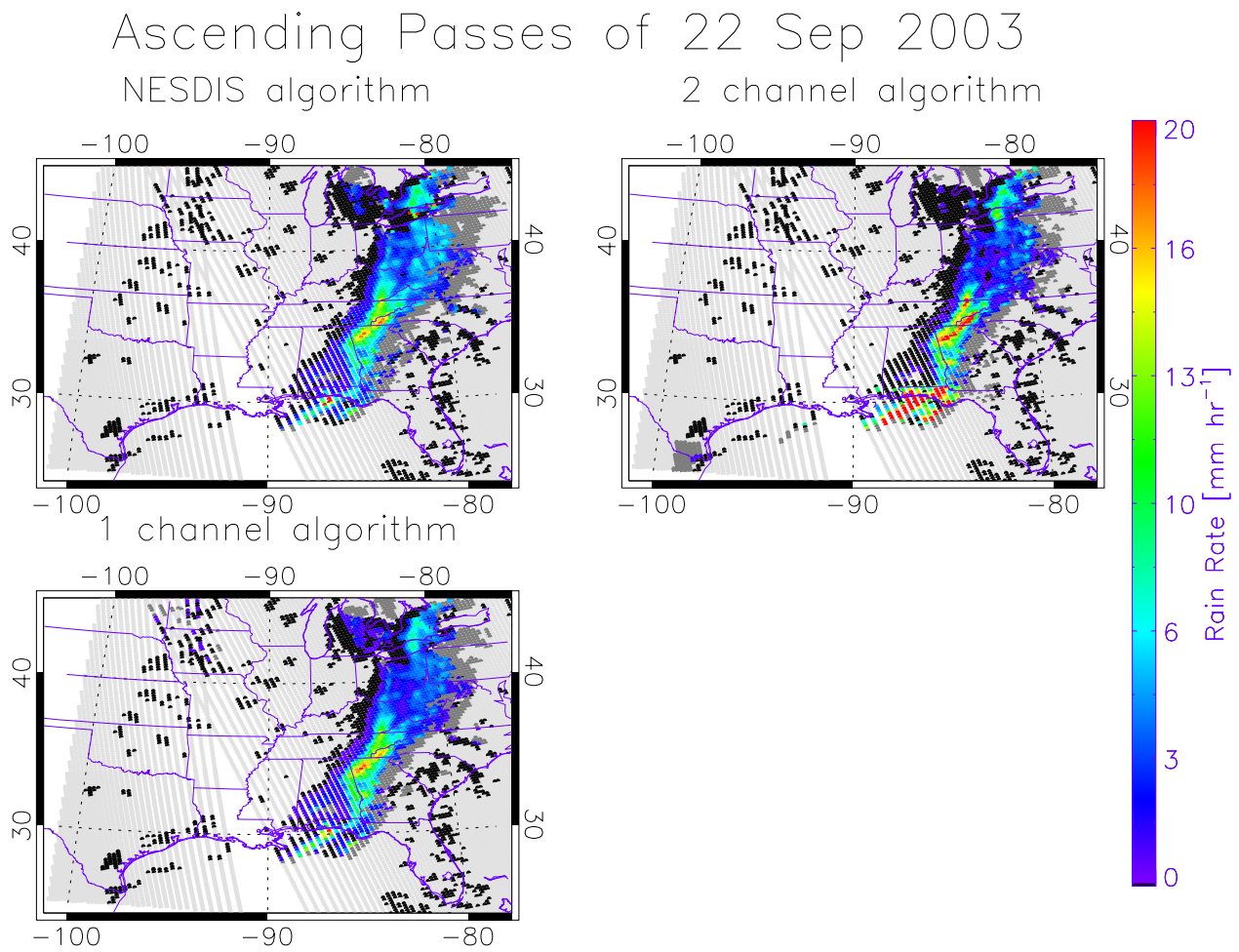

FIG. 2. Visual representation of co-located algorithm and NEXRAD output. Colored areas in the algorithm plots represent AMSU pixels for which the spatially-averaged NEXRAD data also gave a positive rain rate. Black areas represent failed detection by an AMSU algorithm, and dark gray regions represent AMSU-retrieved precipitation that was not present in the radar data.

for the continental United States. Therefore, the results described here cannot be safely extrapolated to more diverse geographic areas. For example, warm-cloud convective processes tend to be more widespread in tropical regions (Petty 1999), and no testing was performed to assess algorithm skill in such regions. It is hypothesized that significant biases would develop if algorithms calibrated to cold-cloud convective activity were applied to other climate regimes.

REFERENCES

Conner, M. D., and G. W. Petty, 1998: Validation and intercomparison of SSM/I rain rate retrieval methods over the continental United States. *Journal of Applied Meteorology*, **37**(7), 679–700.

Ferraro, R. R., and G. F. Marks, 1995: The development of SSM/I rain-rate retrieval algorithms using ground-based radar measurements. *Journal of Atmospheric and Oceanic Technology*, **12**(4), 755–770.

Petty, G. W., 1999: Prevalence of precipitation from warm-topped clouds over Eastern Asia and the Western Pacific. *Journal of Climate*, **12**(1), 220–229.

Weng, F., and N. C. Grody, 2000: Retrieval of ice cloud parameters using a microwave imaging radiometer. *Journal of the Atmospheric Sciences*, **57**(8), 1069–1081.

Zhao, L. M., and F. Weng, 2002: Retrieval of ice cloud parameters using the Advanced Microwave Sounding Unit. *Journal of Applied Meteorology*, **41**(4), 384–395.

Printed August 13, 2004.